Available online at www.sciencedirect.com
SCIENCE DIRECT
Polymer 46 (2005) 12586–12594
polymer
www.elsevier.com/locate/polymer

Miscibility, thermal characterization and crystallization of poly(L-lactide) and poly(tetramethylene adipate-*co*-terephthalate) blend membranes

Ting-Yu Liu [a], Wen-Ching Lin [b], Ming-Chien Yang [b], San-Yuan Chen [a,*]

[a] *Department of Materials Sciences and Engineering, National Chiao Tung University, 1001 Ta-hsueh Road, Hsinchu 300, Taiwan, ROC*
[b] *Department of Polymer Engineering, National Taiwan University of Science and Technology, 43, Sec. 4, Keelung Road, Taipei 106, Taiwan, ROC*

Received 18 October 2004; received in revised form 11 October 2005; accepted 23 October 2005
Available online 11 November 2005

Abstract

Binary blend membranes of biodegradable poly(L-lactide) (PLLA) with poly(tetramethylene adipate-*co*-terephthalate) (PTAT) copolymer were prepared by solution casting via air evaporation. The miscibility of PLLA/PTAT blends was studied by dynamic mechanical analysis (DMA) and thermal mechanical analysis (TMA) in a tensile mode. Differential scanning calorimetry (DSC) measurement was carried out. The surface microstructure and tensile properties of the blend membranes were examined using atomic force microscopy (AFM) and tensile tester. It was concluded that PLLA/PTAT blends should be partially miscible for all ranges of compositions. Higher roughness and porosity were observed for the blend containing 50% PTAT, suggesting more phase separation occurred. The DSC analysis showed that the fusion enthalpy and crystallinity (X_c) of the PLLA-rich phase decreased with increasing PTAT content. Solidification process strongly suggested that the crystallization rate was accelerated by blending with 25% PTAT content, which served as the nucleation agent. Furthermore, the crystallization rate coefficient (CRC) depended on the blending miscibility and cooling rate in the non-isothermal crystallization process. Besides, PTAT addition could be proved to enhance the thermal stability and elongation of resulting blend membranes, even superior to those properties of poly(lactic acid-*co*-glycolic acid) (PLGA).

Keywords: Poly(L-lactide); Poly(tetramethylene adipate-*co*-terephthalate); Blend

1. Introduction

Nowadays, great efforts are devoted to the development of biodegradable materials as potential application for waste management, agriculture, tissue engineering and clinical treatment [1–4]. Biodegradable polymers can be categorized as: (1) naturally occurring polymers from plants, animals and microorganisms, such as cellulose, starch, chitin, and polyhydroxyalkanoates; (2) synthetic polymers, such as polylactide (PLA), poly-(glycolides) (PGA), poly(ε-caprolactone) (PCL), poly(ethylene/butylene succinate); and (3) blends of natural and synthetic polymers, such as starch/PLA systems. Optically active poly(L-lactide) (PLLA) is the semi-crystalline form of PLA. PLLA has been fully employed as a biodegradable drug release carrier [5–7], and also used as artificial scaffold for retinal pigment epithelium as well as other tissue regeneration [8,9]. During metabolization in vivo, PLLA is degraded by hydrolytic de-esterification into lactic acid [10]. The morphology and crystallinity of PLLA strongly influence its rate of biodegradation [11]. However, the commercial application of PLLA is hampered by its hydrophobic, craze and poor processing properties.

There are several approaches can be adapted to improve the properties of PLLA, namely blending and copolymerization. Extensive efforts have been devoted to the study of the effect of the copolymerization of PLA. For instance, the hydrophilicity of the PLA was modified by grafting with poly(ethylene glycol) (PEG) di- or tri-block copolymers [12–14]. Synthetic poly(lactic acid-*co*-glycolic acid) (PLGA) received greater attention and has been currently extensively investigated as a biomaterial for the regeneration of human tissues due to its excellent biocompatibility, mechanical properties and controllable degradation rate [15,16]. In particular, when PLGA are used in drug delivery system, they satisfy such requirements as being non-toxic and biocompatible with no long-term adverse reactions, and are better than other biodegradable polyesters [17]. Although PLGA is a versatile, well characterized material, one great shortcomings is difficult to be

* Corresponding author.
E-mail address: sychen@cc.nctu.edu.tw (S.-Y. Chen).

0032-3861/$ - see front matter © 2005 Published by Elsevier Ltd.
doi:10.1016/j.polymer.2005.10.100

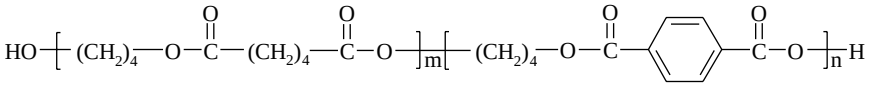

Poly(tetramethylene adipate-co-terephthalate) (PTAT)

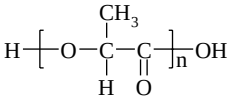

Poly(L-lactide) (PLLA)

Fig. 1. The chemical structure and (a) ^{1}H, (b) ^{13}C NMR spectra of biodegradable PLLA and PTAT copolyesters.

manufactured, which results in a lower supply capacity and higher price.

Blending has been widely and effectively used to modify or control the properties of polymer by appropriately compounding miscible polymers. Miscible polymer blends can create new materials with designated properties, although well-designed miscible polymer blends are rarely found in the literature [18]. On the other hand, immiscibility of blends can generally lead to porous or phase separation structure, which is used for drug release or cell culture [19].

Poly(tetramethylene adipate-*co*-terephthalate) (PTAT) was developed by Eastar Bio company in recent years. Its structure is shown in Fig. 1. PTAT exhibits higher hydrophilicity, better processability than other biodegradable polyesters. In addition, the processability of PTAT is comparable to low density of polyethylene (LDPE) with less ecological problem when disposed. In the literature, miscible and partially miscible blending systems of PLA have been investigated, including PLA/poly(vinylpyrrolidone) [20], PLA/poly(*p*-vinylphenol) [21], PLA/PCL [22], etc. In this present study, PLLA was blended with PTAT to improve its hydrophilicity and processability. The focus of this work is to study the effect of composition on the thermal and mechanical properties and compare with those of PLGA.

2. Materials and methods

2.1. Materials

The PLLA samples used in this study were obtained from Cargill Dow LLC. PTAT (adipic acid:terephthalic acid = 4:3) was purchased from Eastman Corp. Poly(D,L-lactide-*co*-glycolide) (PLGA, lactide:glycolide = 3:1) was obtained from PURAC, Holland. Chloroform was purchased from Acros and used without further purification.

2.2. PLLA/PTAT blend membrane preparations

Blend membranes of various PLLA/PTAT ratios were prepared by solution casting. Chloroform solutions containing 10 wt% polymer of various blending ratios were stirred for 6–8 h at 25 °C and cast on a glass plate. The solution was allowed to evaporate slowly at 25 °C for 6 h. The resulting membranes were then dried at 50 °C for 24 h. PLGA membranes were prepared in the same manner as the characterization control samples. The compositions of all samples are listed in Table 1.

2.3. Surface characterization

The surface morphology was examined using an atomic force microscopy (AFM) (MMAFM-2, Digital Instrument, Santa Barbara, CA). The porosity of the blend membrane was determined by measuring the true density (ρ_t) and the bulk density (ρ_b), as prescribed in our precious study [23]. The porosity (ε) of the sample was calculated according to the equation:

$$\text{Porosity}(\varepsilon) = \frac{1/\rho_b - 1/\rho_t}{1/\rho_b}$$

2.4. Dynamic mechanical characterization

The storage (E') modulus and tan δ of the membranes were measured using a dynamic mechanical thermal analyzer (DMA2980 TA Instruments, USA). The temperature was

Table 1
Glass transition temperature of blend membranes obtained from DMA and TMA peaks and the weight fractions of conjugated phase

Membrane	PLLA (%)	T_g''[a] (°C)	T_g'[a] (°C)	ΔT_g (°C)	W_2'[b]	W_1''[b]	$T_{g,TMA}$ (°C)	α_1 (%/°C)	α_2 (%/°C)
PLLA	100	–	59.1	–			68.4	0.0108	2.12
PLA 75	75	−31.3	50.8	82.1	0.064	0.065	60.3	0.0133	3.52
PLA 50	50	−33.2	57.8	91.0	0.010	0.038	66.9	0.0146	3.36
PLA 25	25	−32.6	54.7[c]	87.3	0.033	0.047	64.1	0.0363	0.699
PTAT	0	−35.8	–	–			–	0.0683	–
PLGA	–	–	40.0	–			50.2	0.0214	13.4

[a] T_g' and T_g'' represented the glass transition temperature of PLLA-rich and PTAT-rich, respectively.
[b] W_2', W_1'' are the weight fraction of PTAT in PLLA-rich and PLLA in PTAT-rich conjugate, respectively.
[c] This T_g was interpolated from the linear correlation between the T_gs from DMA and TMA.

rising from −60 to 150 °C at a heating rate of 5 °C/min, and the oscillation frequency was 1 Hz, and the maximum tensile strain was 0.5%. The glass transition temperature T_g of the samples were obtained from the peak of tan δ curve. The dimensions of the samples were 10×2×1 mm.

2.5. Thermal analysis

The thermal properties of the blends were determined using a differential scanning calorimeter (DSC) (DSC-2910, TA Instruments, USA). In the first heating run, the sample was heated from 25 to 200 °C at a heating rate of 10 °C/min to measure the melting temperature (T_m) and the apparent enthalpy of fusion (ΔH_f). After annealing for 5 min at 200 °C, the sample was cooled to 30 °C at 0.5, 1, 3 or 10 °C/min to determine the crystallization temperature (T_{cc}) and enthalpy (ΔH_{cc}). In the second heating run, the sample was heated from 30 to 200 °C at a heating rate of 10 °C/min. All the DSC measurements were proceeded under N_2 of 10 mL/min. With the aim of determining the thermo-stability of blends, thermogravimetric analysis (TGA-2950, TA Instruments, USA) was used with samples heated from 25 to 800 °C at a heating rate of 10 °C/min in a nitrogen atmosphere. In addition, the thermal expansion coefficient of the membranes was determined using a thermomechanical analyzer (TMA-2940, TA Instruments, USA) from 25 to 80 °C at a heating rate of 10 °C/min.

2.6. The tensile strength and elongation

The tensile strength and elongation of the membrane were measured with a tensile tester (MTS 810, Material Test System, USA) according to ASTM D638M-93. The measurements were taken at room temperature at a crosshead speed of 20 mm/min [23].

3. Results and discussion

3.1. Miscibility of blend membranes

The miscibility of polymers is usually predicted with the solubility parameter δ of the polymers. The solubility parameters can be calculated for any molecule from their constituent functional groups as follows [24,25]:

$$\delta = \left(\frac{\sum E_{coh}}{\sum V}\right)^{1/2} (J^{0.5}/cm^{1.5})$$

where E_{coh} is the molar attraction constant for a particular functional group with volume V. Maximum miscibility will be achieved if the solubility parameters of the two components are identical. When $|\delta_1 - \delta_2|$ is less than 0.5, two polymers may be considered for a miscible solution system [24,26]. The δ's of PLLA and PTAT are 19.70 [27] and 19.83 $J^{0.5}/cm^{1.5}$ (calculated by above equation), respectively. This suggests that PLLA and PTAT are potentially miscible.

3.2. Factors influencing T_g of PLLA–PTAT mixtures

It is well known that T_g is one of the most important indicator for the miscibility of blend components [20–22]. If the two components of a binary blend are miscible in the amorphous phase, only one T_g is expected. The immiscibility of two polymers is demonstrated by the retention of the T_g values of both individual components. If two components are partially miscible, their T_g would shift toward each other [20].

The investigation of relaxation processes of the molecular motions associated with the internal changes can be investigated by dynamic mechanical analysis (DMA). Fig. 2 displayed tan δ curves as a function of temperature for PLGA and PLLA/PTAT blends. The peak temperature of tan δ is used to denote the T_g. Table 1 shows that the T_gs of PLLA, PTAT and PLGA are 59.1, −35.8 and 40 °C, respectively. Those blend membranes exhibited two characteristic peaks. Among them, PLA75 showed partial-miscible with two characteristic peaks at −31.3 and 50.8 °C. These two peaks were closer to each other than those observed between pure PLLA and PTAT. The tan δ peaks of PLA50, at −34.2 and 57.8 °C, were nearly the same as those of neat PLLA and PTAT, respectively. This suggests that the blend membranes with 50% PTAT should be less miscible than PLA75.

Fig. 3 shows the TMA thermograms from 25 to 80 °C of the blend membranes. Because the T_g of PTAT-rich phase is below the temperature limit of the TMA, only the PLLA-rich phase can be observed. Fig. 3 shows that the thermal expansion coefficient α of blend membranes increases with the increase of PTAT content. The maximum α of pure PTAT is 2 and 4.8 times higher than those of PLGA and PLLA, respectively. The TMA curve of PLLA had a turning point at 69 °C, whereas those of PLA75, PLA50 and PLA25 were at 60, 68 and 67 °C, respectively. This suggested that the miscibility of PLA75 was higher than that of PLA25 and PLA50. Therefore, both DMA and TMA results suggest that PLA75 should be more homogeneous than PLA25 and PLA50. Although in Fig. 2, PLA25 has single T_g (−32.6 °C), its TMA thermogram shows a sharp transition at 67 °C in Fig. 3, thus the PLA-rich phase

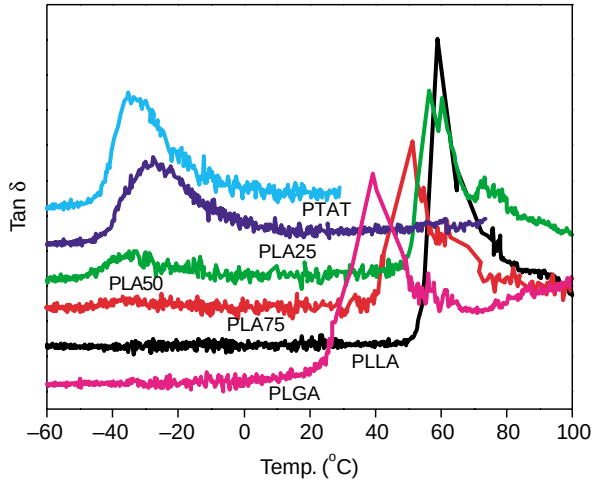

Fig. 2. Tan δ curves of pure and blend membranes measured by DMA.

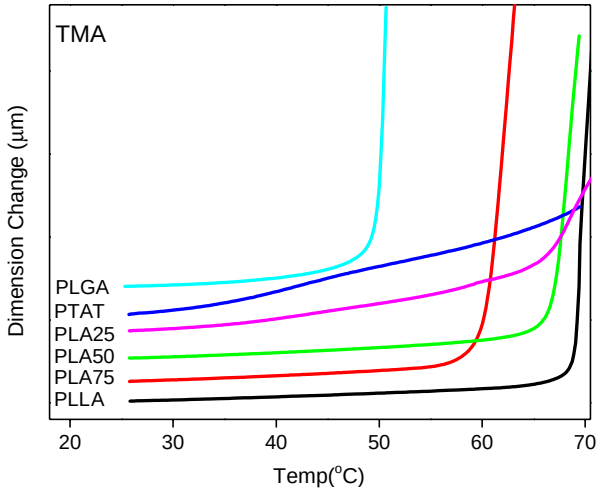

Fig. 3. TMA thermograms of pure and blend membranes.

was still in existence. The disappearance of the second T_g peak was probably because the signal was too small to be observable. Because T_g from TMA is linearly correlated to T_g from DMA ($R^2=0.9998$), the second T_g of PLA25 can be interpolated as 54.7 °C.

For a miscible blend system, the T_g can be described by the Fox equation [28]:

$$\frac{1}{T_g}=\frac{W_1}{T_{g_1}}+\frac{W_2}{T_{g_2}}$$

where W_1 and W_2 are the weight fractions of the compositions, T_{g_1} and T_{g_2} are the T_g of the corresponding blend components. On the other hand, the T_g values in Table 2 cannot be fitted with this simple model. For a partially miscible blend, the composition of conjugated phase can be calculated as follows [18],

$$W_2'=\frac{T_{g_2}(T_{g_1}-T_{g_1}')}{T_g(T_{g_1}-T_{g_2})};\quad W_1''=\frac{T_{g_1}(T_g''-T_{g_2})}{T_g(T_{g_1}-T_{g_2})}$$

where W_i is the weight fraction of component i in blend (1 and 2 designate PLLA and PTAT, respectively), T_g' and T_g'' are the glass transition temperature of pure PLLA and PTAT, respectively, and W_2', W_1'' are the weight fractions of PTAT in PLLA-rich phase and PLLA in PTAT-rich phase, respectively.

The miscibility of PLLA and PTAT can be justified by $\Delta T_g(=T_g{}'-T_g{}'')$ as well as the values of W_1'' and W_2'. Among these three blends, PLA75 had the lowest ΔT_g and highest W_1'' and W_2', whereas PLA50 has the highest ΔT_g and lowest W_1'' and W_2'. Therefore, the order of miscibility is PLA75 > PLA25 > PLA50.

3.3. Blend morphology

In Fig. 4, the AFM topographic images of pure and blend membrane surfaces displayed the microstructures of the surface of the membranes. The blend membranes exhibited larger domains and rougher surfaces than those of pure PLLA and PTAT membranes. Table 2 listed the roughness parameters in both height mode and phase mode. Among these membranes, PLA50 membrane has the maximum phase mode roughness (Rq: 22.4°), whereas the minimum appears in that of PTAT (Rq: 9.67°) and PLLA (Rq: 10.9°). Furthermore, the height mode roughness of PLA50 (Rq: 37.4 nm) was higher than that of PLA75 (22.7 nm) and PLA25 (25.7 nm). The results corresponded with the porosity of blend membranes in Table 2. The maximum porosity (30.7%) appeared in PLA50 blend, whereas the minimum (6.82%) in PTAT membrane. The porosities of PLA75 (22.5%) and PLA25 (13.07%) were close to those of pure PLLA (20.74%) and PTAT. The observation implied that PLA50 had higher phase separation and lower miscibility among the blend membranes.

3.4. Thermal properties of the blend membranes

The TGA measurement results, as showed in Fig. 5, indicated that both PLLA and PTAT are stable when heating temperature is less than 300 °C. Above 300 °C, the PLLA degraded to 90% at 323 °C and 50% at 351 °C, whereas PTAT degraded to 90% at 370 °C and 50% at 396 °C. In comparison, PLGA degraded to 90% at 283.0 °C and 50% at 353.2 °C. This suggested the PTAT had better thermo-stability than PLLA and PLGA. Thus blending PLLA with PTAT can efficiently improve the thermal stability.

The DSC thermograms of PLLA, PTAT and PLGA obtained from heating and cooling cycles at 10 °C/min are shown in Fig. 6. In the first heating run, pure PLLA displayed a relatively sharp melting endotherm enthalpy (ΔH_f) of 47.14 J/g at 170 °C, while PTAT displayed a broad temperature peak at 108 °C with a lower melting enthalpy (10.82 J/g), which was similar to that of PLGA (9.29 J/g) at 83 °C. This suggests that PTAT is more amorphous than PLLA.

In Fig. 6(b), there is no distinct crystallization peak (T_{cc}) for PLLA and PLGA in the non-isothermal solidification process at a cooling rate 10 °C/min. Sheth et al. [29] also

Table 2
Roughness of blend membrane by AFM and porosity of blend membranes

Membrane	Height mode (nm)	Phase mode (°)	True density (ρ_t) (g/cm^3)	Bulk density (ρ_b) (g/cm^3)	Porosity (%)
PLA100	22.65	10.91	1.443	1.142	20.74
PLA75	27.66	16.06	1.389	1.076	22.50
PLA50	37.39	22.38	1.372	0.951	30.70
PLA25	25.71	13.68	1.201	1.044	13.07
PTAT	21.01	9.67	1.284	1.196	6.82

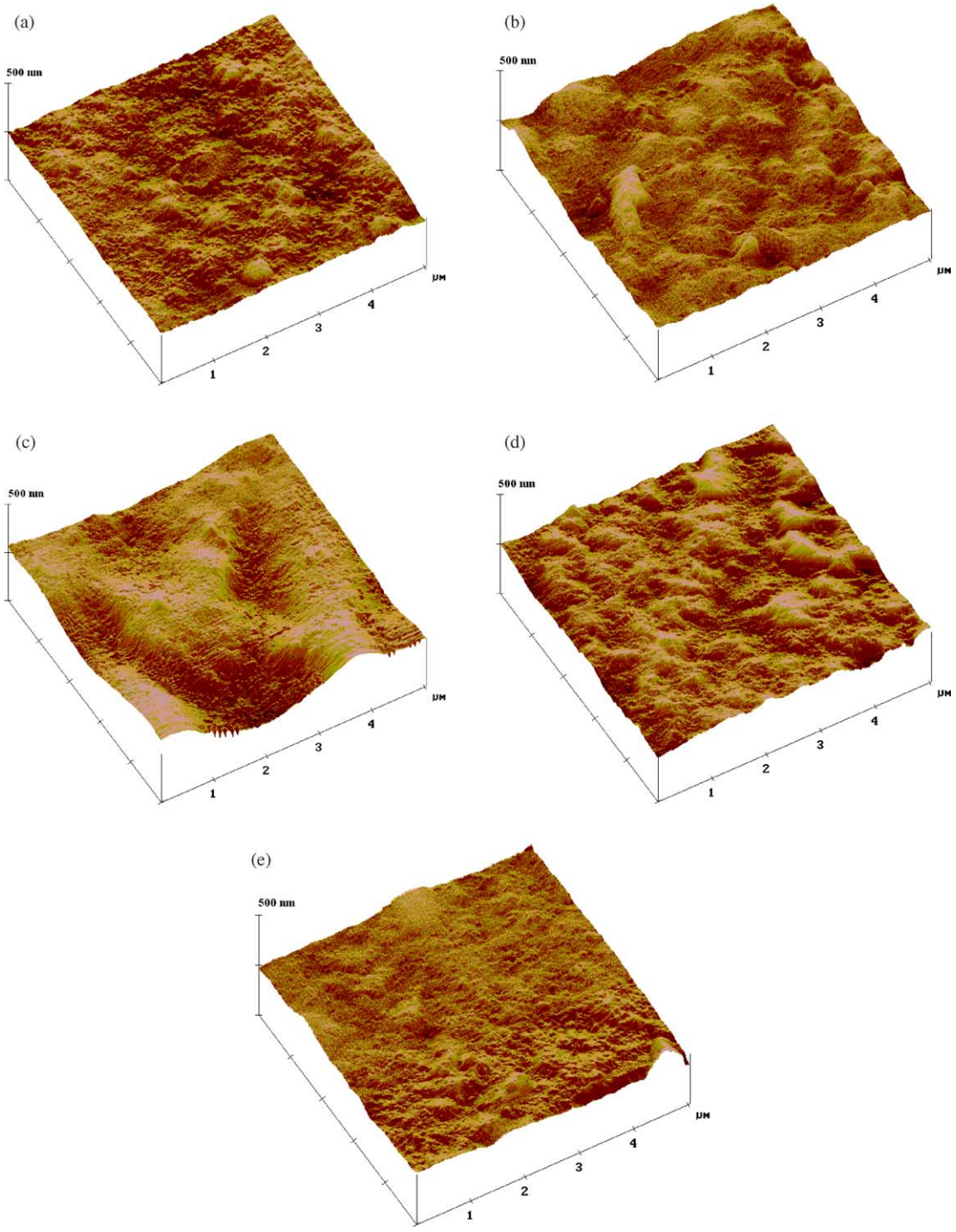

Fig. 4. AFM topographic images of pure and blend membrane surfaces: (a) PLLA; (b) PLA75; (c) PLA50; (d) PLA25; (e) PTAT.

reported that there is no crystallization exotherm peak for pure PLA at this cooling rate. However, the T_{cc} peak of PLLA became sharper at lower cooling rates, as shown in Fig. 6(c). On the other hand, the T_{cc} peak of PTAT appeared at 75.9 °C with an exotherm enthalpy (ΔH_{cc}) of 12.9 J/g cooling at 10 °C/min, but became smaller in peak area at slower cooling rates, as shown in Fig. 6(d). This suggests that PTAT has a higher crystallization rate in non-isothermal process than those of PLLA and PLGA.

The half-height widths of the crystallization peaks (ΔT_{cc}) were listed in Table 3. The values of ΔT_{cc}, for the blends were considerably higher than for pure PLLA. Furthermore, ΔT_{cc} of pure PLLA decreased with the increase of cooling rate. On the contrary, ΔT_{cc} of pure PTAT increased with the increase of cooling rate.

Fig. 7 shows the DSC theromgrams for a series of PLLA/PTAT blends. It is well known that the T_m of the crystalline component in a polymer blend depends on both morphological

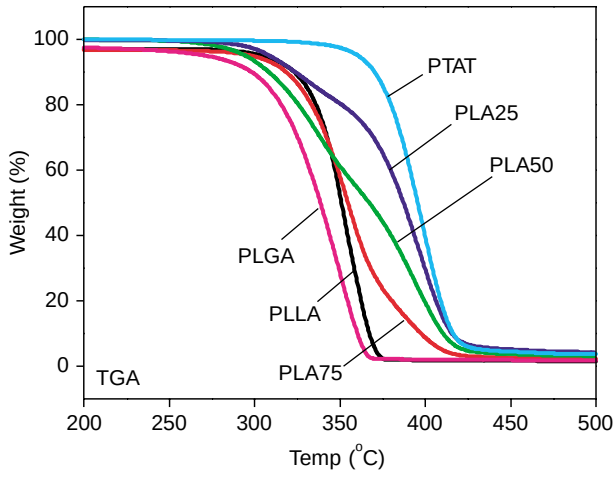

Fig. 5. TGA thermograms of pure and blend membranes.

and thermodynamic factors [30]. In case of miscible blends with amorphous polymers, the thermodynamic factor would result in the depression of T_m. As shown in Table 4, the T_m of PLLA decreased with the increase of PTAT content. In addition, ΔH_f decreased with the increase of PTAT content. The crystallinity, X_c, was calculated as follows [20]:

$$X_c = \frac{\Delta H_f}{\Delta H_f^0 \omega W_1'}$$

where ΔH_f is the apparent enthalpy of fusion (indicated in DSC thermograms as the melting enthalpy per gram of blends) corresponding to the component, ω is the total weight fraction of the PLLA in the blend, $W_1'(=1-W_2')$ is the weight fraction of PLLA in PLLA-rich phase, and ΔH_f^0 is the enthalpy of fusion per gram of the component in its completely crystalline state (93 J/g for PLLA) [22].

From the date in Table 4, we noted that X_c of PLLA-rich phase decreased more for PLA75 (37.8%) than for PLA50 (39.1%) and PLA25 (38.9%) blend membranes. It is well known that for polymer blends containing a semi-crystalline component, the variations in the values of X_c are usually due to the interactions between components [21]. Therefore, the decrease in X_c for PLLA/PTAT blends implies that PLLA and PTAT are partially miscible, and the miscibility of PLA75 is higher than other blend ratios due to the higher decrease in X_c.

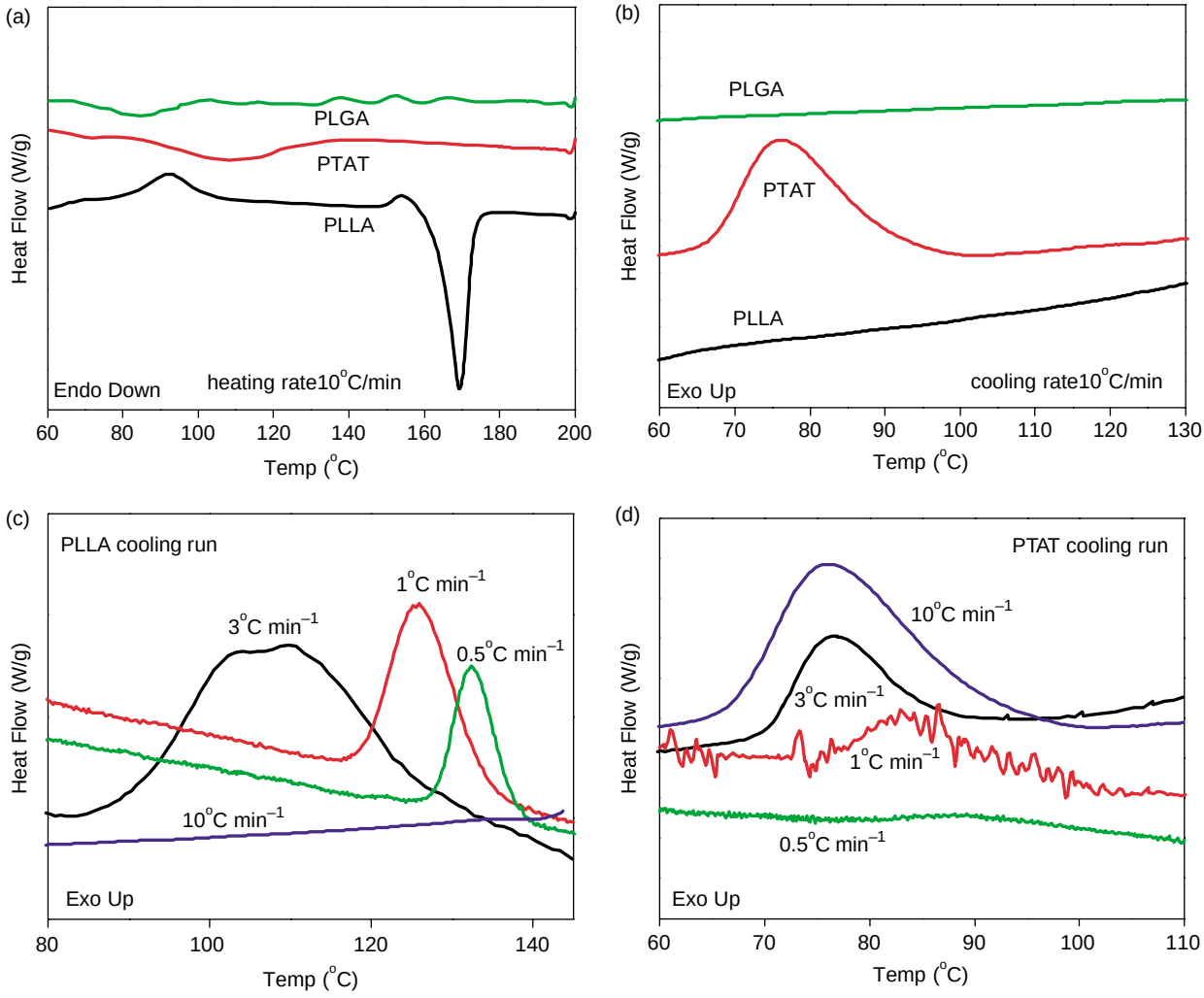

Fig. 6. DSC thermograms of pure membranes (PLLA, PTAT, PLGA), including heating process and non-isothermal cold process.

Table 3
Non-isothermal cooling process of PLLA/PTAT blend membranes from DSC measurement

No.	Blend	$\chi = 0.5$ °C min^{-1}				$\chi = 1$ °C min^{-1}				$\chi = 3$ °C min^{-1}				CRC (h^{-1})
	PLLA/PTAT	T_{cc} (°C)	ΔT_{cc} (°C)[a]	ΔH_{cc} (J/g)	ΔT (°C)[b]	T_{cc} (°C)	ΔT_{cc} (°C)[a]	ΔH_{cc} (J/g)	ΔT (°C)[b]	T_{cc} (°C)	ΔT_{cc} (°C)[a]	ΔH_{cc} (J/g)	ΔT (°C)[b]	
PLLA	100/0	132.3	5.67	22.67	73.2	125.8	8.61	19.69	66.7	109.7	23.83	16.23	50.6	6.79
PLA 75	75/25	115.9	12.59	25.98	65.1	112.8	12.88	25.87	62	98.8	16.11	12.56	47.3	8.71
PLA 50	50/50	121.8	17.84	13.6	64	113.2	14.63	15.09	55.4	101.5	15.97	8.09	43.7	7.55
PLA25	25/75-PLLA[d]	–	–	–	–	111.3	5.14	5.62	–	–	–	–	–	–
	25/75-PTAT[d]	89.78	3.04	1.85	–	81.1	10.13	5.89	–	76.2	8.95	3.05	–	10.17
PTAT	0/100	90.18	14.53	6.34	–	83.3	12.41	8.47	–	76.4	9.18	10.11	–	10.89
PLGA[c]	–	–	–	–	–	–	–	–	–	–	–	–	–	–

[a] ΔT_{cc} = half-height width of the T_{cc} peak.
[b] $\Delta T = T_{cc} - T_g$.
[c] The T_{cc} peak of PLGA membrane are not conspicuous.
[d] The 25/75-PLLA and 25/75-PTAT mean the T_{cc} peak in PLLA-rich and PTAT-rich phase, respectively.

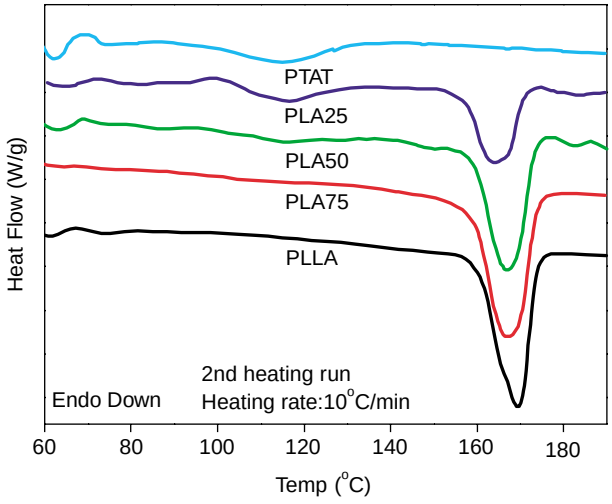

Fig. 7. DSC thermograms of pure and blend membranes in first and second heating cycles.

3.5. Non-isothermal crystallization kinetic

Although PLLA is an engineering plastic offering excellent thermal and chemical resistance, mechanical strength and biodegradability, it is seldom considered for applications involving high-speed processing such as injection molding because it is a high-melting and slow-crystallizing polymer. The influence of the PTAT content on the dynamic solidification of PLLA/PTAT blends is shown in Fig. 8. The addition of 25% PTAT shifted the crystallization peak to a lower temperature. Zhang et al. [21] used a characteristic temperature $\Delta T(=T_{cc}-T_g)$ to describe the kinetic crystallizability and crystallization rate during the non-isothermal crystallization process. Higher ΔT means lower kinetic crystallizability from T_g to T_m range. As shown in Table 3, ΔT of PLA75 (62.0 °C) and PLA50 (55.4 °C) were lower than that of PLLA (66.7 °C), thereby suggested the blend had higher kinetic crystallizability and crystallization rate than pure PLLA. Thus the overall non-isothermal crystallization kinetics of PLLA would be accelerated by blending PTAT. In other words, PTAT accelerates the nucleation and growth process of PLLA in a manner similar to that of a nucleating agent. That is, those PTAT amorphous domains appear to serve as the effective nucleation sites for PLLA, as suggested by the higher nucleation density in the blends. Ou et al. [31] have investigated the crystallization behavior of poly(oxybenzoate-*p*-butylene terephthalate) copolymer blending with

Table 4
Melting behavior of PLLA/PTAT blend membranes (second heating run)

Membrane	T_m (°C)[a]	ΔT_m (°C)[b]	ΔH_f (J/g)	X_c (%)
PLLA	169.3	8.42	43.44	46.7
PLA75	167.2	9.83	24.66	37.8
PLA50	166.7	9.11	18.01	39.1
PLA25	163.8	9.39	8.64	38.9
PTAT	114.9	21.09	7.01	–

[a] Non-isothermal solidification at a heating rate of 10 °C/min.
[b] ΔT_m is the half-height width of the T_m peak.

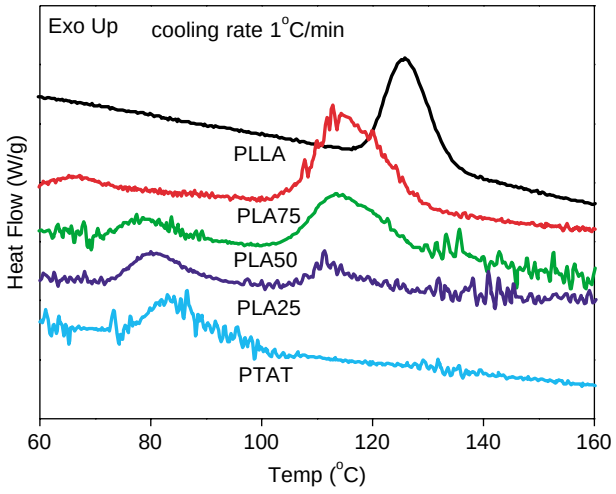

Fig. 8. DSC thermograms of pure and blend membranes in non-isothermal cold cycle at a cooling rate of 1 °C/min.

poly(ethylene terephthalate) (PET) and showed that the crystallization rate of PET was accelerated by blending with 1–15 wt% copolymer. Sharma et al. [32] studied PET/liquid crystalline polymer (LCP) blend and proposed that LCPs act like nucleating agents for PET crystallization and the effect probably reached a maximum LCP addition between 1 and 5 wt%.

The cooling rate in the non-isothermal solidification process also played a very important role in the crystallization of PLLA/PTAT blends. For neat PLLA and PTAT with decreasing cooling rate, the crystallization peaks shifted to higher temperatures, as shown in Fig. 6(c) and (d). It can be explained that at lower cooling rate there is more time to overcome the nucleation barrier, thus the crystallization started at higher temperature. Therefore, the T_{cc} of PLLA could not be detected at 10 °C/min, but appeared in 125.8 °C at 1 °C/min. Khanna [33,34] introduced a crystallization rate coefficient (CRC) defined as the variation in cooling rate required for a 1 °C-change in the

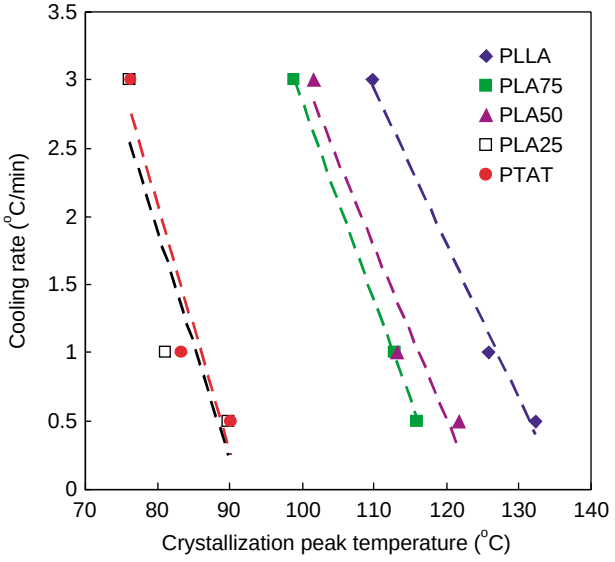

Fig. 9. A comparison of the CRC values of PLLA/PTAT blend membranes.

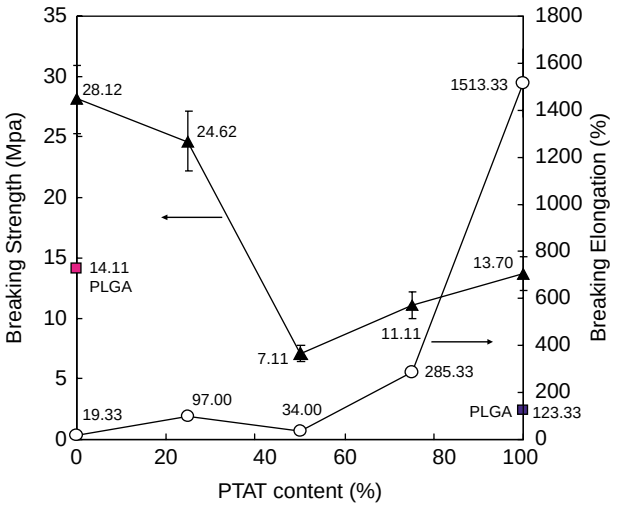

Fig. 10. The mechanical properties of PLLA/PTAT blend membranes.

undercooling of the polymer melt. The CRC can be measured from the slope of the plot of cooling rate versus crystallization peak temperature and can be used as a guide for ranking the polymers on a scale of crystallization rates. Higher CRC means faster crystallizing. A comparison of the CRC values was shown in Fig. 9. In general, the CRCs of PLLA/PTAT blend membranes increased with the PTAT content, as shown in Table 3. In particular, the CRC of PLA75 (8.71 h^{-1}) was slightly higher than that of PLA50 (7.55 h^{-1}). This may be because the miscibility of PLA75 was better than PLA50.

3.6. Mechanical properties of the blends

Fig. 10 shows the mechanical properties of PLLA/PTAT blend membranes. Tensile strength at break was, respectively, 28 and 14 MPa for PLLA and PTAT. The breaking elongation was 19 and 1513% for PLLA and PTAT, respectively. The results suggest that PLLA is hard and brittle, whereas PTAT is more ductile. The tensile strength of blends decreased with the increase of the PTAT content, yet with 50% PTAT the tensile strength dropped by 75% (7 MPa). The breaking elongation exhibited similar trend. The inflection of elongation of blends appeared for PLA50. This could be due to poor-miscibility and higher phase separation in PLA50 blend. Furthermore, the breaking elongation of PLA75 (97%) was about times times higher than that of PLLA (19%). The results were consisted with the Nijenhuis et al. [11]. They have been proposed that higher PEO concentrations up to 20% in PLLA make the materials more flexible, and the breaking elongation of more than five times of that of PLLA. It would be worthy noting that the mechanical properties of PLA75 (25 MPa, 97%) and PLA25 (11 MPa, 285%) were more comparable to that of PLGA (14 MPa, 123%) than those of PLLA (28 MPa, 19%).

4. Conclusions

A series of PLLA and PTAT blend membranes were prepared. The miscibility, microstructure, thermal

characterization and crystallization behavior of these blends were investigated by DMA, AFM and DSC, respectively. It is concluded that the blend membrane with 25% PTAT (PLA75) exhibited higher miscibility and higher tensile strength than other blend ratios. Furthermore, the crystallization rate coefficients of the blend membranes were higher than the original PLLA. By blending with PTAT, the mechanical strength and elongation of PLLA could be improved and comparable to those of PLGA. Therefore, biodegradable polyester blending of PLLA with PTAT cannot only be a convenient approach to improve the thermal stability, tensile properties and crystallization, but also be comparable to those of much expensive PLGA. Based on this preliminary study, the investigation for biodegradability, drug controlled release, and cytocompatibility of PLLA/PTAT blend membranes is now in progress in this group.

References

[1] Hu Y, Zhang C, Zhang S, Xiong Z, Xu J. J Biomed Mater Res 2003;67A: 591.
[2] Hutmacher DW. Biomaterials 2000;21:2529.
[3] Na YH, He Y, Shuai X, Kikkawa Y, Doi Y, Inoue Y. Biomacromolecules 2002;3:1179.
[4] Hu SG, Jou CH, Yang MC. Biomaterials 2003;24:2685.
[5] Kubies D, Rypacek F, Kovarova J, Lednicky F. Biomaterials 2000;21: 529.
[6] Nguyen K, Su T, Sheng SH, Wawro A, Schwade D, Brouse ND, et al. Biomaterials 2003;24:5191.
[7] Jain R, Shah NH, Malick AW, Rhodes CT. Drug Dev Ind Pharm 1998;24: 703.
[8] Kim SY, Kanamori T, Noumi Y, Wang PC, Shinbo T. J Appl Polym Sci 2004;92:2082.
[9] Kim K, Yu M, Zong X, Chiu J, Fang D, Seo YS, et al. Biomaterials 2003; 24:4977.
[10] Liu L, Li S, Garreau H, Vert M. Biomacromolecules 2000;1:350.
[11] Nijenhuis AJ, Colstee E, Grijpma DW, Pennings AJ. Polymer 1996;37: 5849.
[12] Liu L, Li C, Li X, Yuan Z, An Y, He B. J Appl Polym Sci 2000;80:1976.
[13] Khaled AA, Heidi S, Surita RB, Gregory NT. Biomaterials 2004;25:1087.
[14] Li YX, Kissel T. J Controlled Release 1993;27:247.
[15] Jain RA. Biomaterials 2000;21:2475.
[16] Gumusderelioglu M, Deniz G. J Biomater Sci Polym Ed 2000;11:1039.
[17] Dunn RL. In: Hollinger JO, editor. Biomedical applications of synthetic biodegradable polymers. Boca Raton, FL: CRC Press; 1995. p. 17.
[18] Kim BK, Oh YS, Lee YM, Yoon LK, Lee S. Polymer 2000;41:385.
[19] Rahman NA, Mathiowitz E. J Controlled Release 2004;94:163.
[20] Zhang G, Zhang J, Zhou X, Shen D. J Appl Polym Sci 2003;88:973.
[21] Zhang L, Goh SH, Lee SY. Polymer 1998;39:4841.
[22] Na YH, He Y, Shuai X, Kikkawa Y, Doi Y, Inoue Y. Biomacromolecules 2002;3:1179.
[23] Yang MC, Liu TY. J Membr Sci 2003;226:119.
[24] Van Krevelen DW. Properties of polymers. Amsterdam: Elsevier Scientific, 2nd ed 1976 p. 129.
[25] Slark AT. Polymer 1997;38:2407.
[26] Yin X. J Membr Sci 1998;146:179.
[27] Kiss E. J Colloid Interface Sci 2002;245:91.
[28] Fox TF. J Appl Bull Am Phys Soc 1956;1:123.
[29] Sheth MS, Kumar RA, Dave V, Gross RA, Mccarthy ST. J Appl Polym Sci 1997;66:1495.
[30] Coleman MM, Graf JF, Painter PC. Specific interactions and the miscibility of polymer blends. Lancaster, PA: Technomic Publishing; 1991.
[31] Ou CF, Huang SL. J Appl Polym Sci 2000;76:587.
[32] Sharma SK, Tendokar A, Misra A. Mol Cryst Liq Cryst 1988;157:597.
[33] Khanna YP. Polym Eng Sci 1990;30:1615.
[34] Minkova LI. Polymer 1995;36:2059.